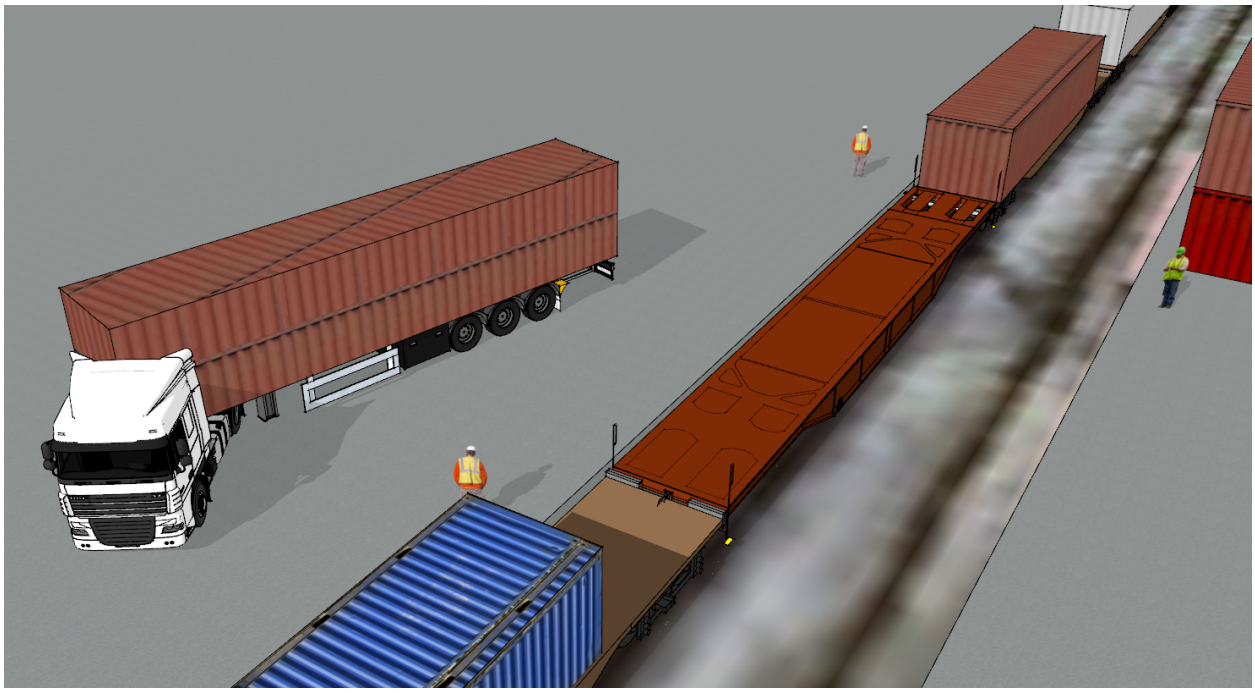
CHALMERS
UNIVERSITY OF TECHNOLOGY



Assisted precision maneuvering of truck and semi-trailer onto a railway wagon

Proof of Concept implementation of a system for assisted reverse maneuvering of truck and semi-trailer combinations

Master's thesis in Mobility Engineering

HARSHITH PIDUR KUPPUSAMY & RADU RAZNOVAN

DEPARTMENT OF MECHANICS AND MARITIME SCIENCES

CHALMERS UNIVERSITY OF TECHNOLOGY
Gothenburg, Sweden 2026
www.chalmers.se

Master's thesis 2026

Assisted precision maneuvering of truck and semi-trailer onto a railway wagon

Proof of Concept implementation of a system for assisted reverse maneuvering of truck and semi-trailer combinations

HARSHITH PIDUR KUPPUSAMY
RADU RAZNOVAN



CHALMERS
UNIVERSITY OF TECHNOLOGY

Department of Mechanics and Maritime Sciences
Division of Vehicle Engineering and Autonomous Systems
Chalmers University of Technology
Gothenburg, Sweden 2026

Assisted precision maneuvering of truck and semi-trailer onto a railway wagon

HARSHITH PIDUR KUPPUSAMY
RADU RAZNOVAN

© HARSHITH PIDUR KUPPUSAMY & RADU RAZNOVAN, 2026.

Supervisor: Zhaohui Ge, Doctoral student, Vehicle Engineering and Autonomous Systems, Mechanical Engineering
Examiner: Fredrik Bruzelius, Director of Studies, Mechanical Engineering

Master's Thesis 2026
Department of Mechanics and Maritime Sciences
Division of Vehicle Engineering and Autonomous Systems
Chalmers University of Technology
SE-412 96 Gothenburg
Telephone +46 31 772 1000

Cover: Sketch-up visualization of a truck in a railway terminal.

Chalmers Digital Printing
Gothenburg, Sweden 2026

Assisted precision maneuvering of truck and semi-trailer onto a railway wagon.

HARSHITH PIDUR KUPPUSAMY
RADU RAZNOVAN
Department of Mechanics and Maritime Sciences
Division of Vehicle Engineering and Autonomous Systems
Chalmers University of Technology

Abstract

Intermodal transport has gained increasing attention in recent years as a means of combining multiple modes of freight transport — typically road, rail, and sea, to lower emissions from road based logistics. One approach to road-rail transshipment is horizontal Ro-Ro (Roll-on/Roll-off) loading, in which a tractor and semi-trailer reverses directly onto a rail wagon without the need for crane lifting or specialized trailer reinforcement.

The maneuver requires the driver to reverse the combination in a constrained area, align the trailer precisely with the wagon, and complete the final docking at a near-perpendicular angle between the tractor and trailer — all within tight lateral tolerances and often without dedicated sensing or guidance infrastructure. Precision reverse maneuvering of articulated truck-trailer combinations is inherently challenging due to limited rearward visibility, instability of the articulation angle during reverse motion, and the vehicle's nonholonomic constraints, making the repeatable execution of such maneuvers difficult even for experienced drivers. In space-constrained environments such as road-to-rail intermodal terminals, maneuvering errors can lead to delays and safety risks, ultimately reducing the throughput of the transshipment process.

This thesis presents a framework for implementing a driver assistance system designed to reduce the time and workload associated with horizontal Ro-Ro loading maneuvers. The proposed solution integrates four subsystems: a LiDAR-based perception pipeline, a path planner, a path-following controller, and a driver user interface. The framework is implemented in Simulink and enables closed-loop operation on a real vehicle.

Results confirm that the proposed approach is technically feasible and that the individual subsystems function as intended, with limitations related to real-time LiDAR data streaming, and articulation angle control identified as areas requiring further development.

Keywords: LiDAR, vehicle detection, path planning, path following control

Acknowledgements

We would like to thank our external supervisor Hanns Hallesius and the team at Tructric AB for providing us the opportunity to undertake this project and being supportive through all the setbacks and challenges.

We thank our Chalmers supervisor Zhaohui Ge and Examiner Fredrik Bruzelius for offering continuous help, clarifications and suggestions.

Special thanks to Daniel Poveda Pi, Tommi Saarikoski, Fredrik Von Corswant at REVERE lab for providing us the tools, opportunities to perform tests with 'Elephant'- an Volvo FHE truck.

Harshith & Radu
Gothenburg, Sweden 2026

List of Acronyms

Below is the list of acronyms that have been used throughout this thesis listed in alphabetical order:

bvp4c	Boundary Value Problem Solver
BBIOM	Body Builder Input-Output Model (Volvo)
CAN	Controller Area Network
DAS	Driver-assistance system
DBC	Database Container file (for decoding CAN-bus signals)
DBSCAN	Density-based spatial clustering of applications with noise
EXSTER	Volvo Trucks External Steering Interface
FHE and FME	Variants in Volvo 'FH' and 'FM' series trucks
FOV	Field of View
GNSS	Global Navigation Satellite System
GPS	Global Positioning System
IMU	Inertial Measurement Unit
LiDAR	Light Detection and Ranging
LCV	Long Combination Vehicles
LQR	Linear Quadratic Regulator
OEM	Original Equipment Manufacturer
PCA	Principal component analysis
PCAP	Packet Capture file format
PID	Proportional-Integral-Derivative control
RADAR	Radio Detection and Ranging
RANSAC	Random sample consensus
Ro-Ro	Roll-on/Roll-off
RRT	Rapidly Exploring Random Trees
RTK	Real Time Kinematic

Nomenclature

Below is the nomenclature of indices, sets, parameters, and variables that have been used throughout this thesis.
All angles are measured positive in counter-clockwise direction, in radians unless mentioned otherwise.

Indices

i,j	Indices for 1D or 2D arrays
t	Index for time step

Sets

$\mathcal{X}_s$	State vector defining start pose of vehicle
$\mathcal{X}_g$	State vector defining goal pose of vehicle

Parameters

M	Hitch point off axle distance from tractor rear axle [m]
L_1	Tractor wheelbase (front axle to rear equivalent axle) [m]
L_2	Distance from hitch point to semi-trailer equivalent axle [m]
α_{max}	Allowed maximum road wheel angle [rad]
β_{max}	Allowed maximum articulation angle [rad]

Variables

α	Road wheel angle [rad]
κ	Curvature [1/m]

σ	Driving direction scalar (+1 for forward, -1 for reverse)
θ_1	Heading angle of tractor [rad]
θ_2	Heading angle of trailer unit [rad]
β	Articulation angle between tractor and trailer units [rad]
v_{11}	Velocity of tractor front axle [m/s]
v_{12}	Velocity of tractor rear equivalent axle [m/s]
v_{21}	Velocity of hitch point [m/s]
v_{22}	Velocity of semi-trailer rear equivalent axle [m/s]
S	Path distance [m]

Contents

List of Acronyms vii

Nomenclature viii

List of Figures xii

List of Tables xiii

1 Introduction 1
- 1.1 Background . . . 1
- 1.2 Motivation . . . 2
- 1.3 Existing driver assist for reversing . . . 2
- 1.4 Objectives and limitations . . . 4

2 Sensing 5
- 2.1 Setup . . . 6
- 2.2 Field data gathering . . . 7
- 2.3 Methods and algorithms for point cloud processing . . . 8

3 Modeling and Path planning 11
- 3.1 Kinematic Model . . . 11
  - 3.1.1 Model validation using TruckMaker™ simulations . . . 14
- 3.2 Computational methods for path planning . . . 15
  - 3.2.1 Commonly used methods . . . 15
  - 3.2.2 Direct collocation algorithm . . . 17
- 3.3 Path following control . . . 20
  - 3.3.1 Controller Architecture . . . 20

4 Vehicle testing 21
- 4.1 Test vehicle setup . . . 21
- 4.2 EXSTER Interface . . . 22
- 4.3 Objectives and limitations . . . 23

5 Results and discussion 25
- 5.1 LiDAR . . . 25
  - 5.1.1 Results . . . 25
  - 5.1.2 Challenges . . . 25

5.2 Path planner 26
5.2.1 Output 26
5.3 Path following controller 28
5.3.1 Extending reference path 28
5.3.2 Look-ahead distance and stability 28
5.3.3 Articulation angle control 30
5.4 Outcomes of Testing 31

6 Conclusion and future work **36**
6.1 Conclusion 36
6.2 Future Work 37
6.2.1 Terminal articulation angle control 37
6.2.2 Improvements in LiDAR processing 37
6.2.3 Camera based identification and position estimation 37
6.2.4 User interface 37

Bibliography **39**

List of Figures

1.1 Conventional equipment used in road-rail intermodal shipment 1
1.2 Parking maneuver on a mock-up railway wagon (*Source:Tructric AB*) 2
1.3 Concept flowchart 4

2.1 LiDAR used to collect data 7
2.2 Truck and trailer view from LiDAR recordings [15] 8
2.3 High-level overview of LiDAR sensing logic 9
2.4 Localization using LiDAR point cloud 10

3.1 Kinematic model schematic (drawn for M<0) 11
3.2 Model validation with handwheel angle of 1 rad 14
3.3 Model validation with handwheel angle of 12.5 rad 14

4.1 REVERE 'Elephant' [25] 21

5.1 Annotated view of a truck and trailer, illustrating challenges in LiDAR-based perception 26
5.2 Path planner output with way-point 27
5.3 Path planner output without way-point 27
5.4 Padding added to trailer reference path 28
5.5 Example of path tracking performance with balanced look-ahead distance 29
5.6 Example of path tracking performance with shorter look-ahead distance 29
5.7 Example of path tracking performance with longer look-ahead distance 30
5.8 Convergence of rear axle to target point 30
5.9 Manual straight line reverse 32
5.10 Constant steering angle reverse close to jackknife 33
5.11 Simulated Ro-Ro parking on test platform 34

List of Tables

2.1 Sensing methods explored 5
2.2 VLP-16 Specification 7

3.1 Variables and parameters of the kinematic single track model 13
3.2 Selected parameter values used in the path planner 17

4.1 Logged data for each maneuver 22

5.1 Comparison of path planner performance with and without way-point 27
5.2 RMS of position errors 35

1
Introduction

1.1 Background

Road freight handled by heavy trucks contributes roughly 25-36% of the total road transport CO_2 emissions in Sweden, which accounts for 6.5-7% of total greenhouse emissions in the country [1] [2] - A similar trend applies for the European Union as a whole. With increasing legislation pushing the transport sector to reduce emissions and possibly achieve net zero by 2045, it is worthwhile to consider methods for making long distance freight shipment more energy efficient.

One widely discussed strategy for reducing the emissions from long distance freight is intermodal transport, i.e. leveraging existing electrified rail infrastructure for the main haul, with trucks handling only the first and last legs of the journey. Between 2014 and 2025, heavy vehicle freight transport data from Sweden shows a stable freight volume, ranging from 38.1 to 45.8 billion tonne-kilometres [3]. Reducing the total tonne-kilometers of road transport ultimately would lead to a lower contribution of greenhouse emissions from the transport sector.

As of 2026, the majority of the semi-trailers in Europe remain incompatible with conventional intermodal terminal handling. Standard terminal operations rely on crane lifting or reach stackers (Figure 1.1), and only an estimated 10% of semi-trailers in the EU are structurally reinforced to be liftable [4].



(a) Reach stacker [5] **(b)** Gantry crane [6]

Figure 1.1: Conventional equipment used in road-rail intermodal shipment

A compelling alternative is horizontal Ro-Ro (Roll-on/Roll-off) loading, in which a semi-trailer is driven directly onto a rail wagon without any lifting equip-

ment or requiring special structural reinforcement of the trailer. This approach, based on precision maneuvering, is compatible with the full semi-trailer fleet and eliminates the need for dedicated crane infrastructure at terminals.

The trailer loading system proposed by Tructric AB falls under the horizontal assisted Ro-Ro transshipment category. Notably, it does not require any modification of the existing terminal infrastructure [7], which improves accessibility and competitiveness of rail-road intermodal transportation. Topics related to the method to secure the kingpin (hitch), and cost of implementation are not addressed here as they are beyond the scope of this thesis.

1.2 Motivation

Reverse parking Ro-Ro maneuvers, for parking a semi-trailer onto a loaded bed of a railway wagon with precision, place significant demands on the driver: precisely aligning and reversing a tractor and semi-trailer combination onto a rail wagon within tight lateral tolerances is a complex task that currently depends entirely on driver skill. During field testing, it was observed that even skilled drivers found it challenging to perform such maneuvers with good repeatability.

This motivates the development of a driver assist system with sensors and driver in loop, capable of automating or guiding the Ro-Ro docking maneuver. The particular type of maneuver to be performed to load a semi-trailer onto a rail wagon is shown in Figure 1.2 as reference.



(a) Front View **(b)** Side View

Figure 1.2: Parking maneuver on a mock-up railway wagon (*Source:Tructric AB*)

1.3 Existing driver assist for reversing

Existing driver-assist functionality for reversing is limited. For this thesis, driver-assist capability for reverse precision maneuvering that incorporates local path planning was identified as a gap.

In contrast, several auxiliary sensing technologies are already used in the transport sector to support reversing by providing warnings, visual overlays, or general quality-of-life improvements. Examples of commonly used sensors that provide additional information to the driver during reversing include:

1. Blind spot monitoring cameras - provides visual coverage of areas not visible in mirrors.
2. Magnetic wireless cameras - temporary or portable cameras mounted on the trailer for improved rear visibility.
3. Radar or ultrasonic parking sensors - detect nearby obstacles and provide proximity warnings.

While camera-based reversing aids can provide useful trajectory overlays for non-articulated vehicles, their effectiveness is questionable for articulated configurations [8], where the hitch dynamics introduce non-intuitive motion that cannot be reliably inferred from a single viewpoint. As a result, drivers must still rely heavily on experience and intuition, limiting the practical value of camera-only solutions in articulated reversing scenarios.

There is a clear need for a guidance system with path-planning and path-following control for tractor–semi-trailer combinations during precision reversing. Such a system can reduce the time required to complete a reverse maneuver, enable drivers with beginner or intermediate experience to perform these maneuvers with fewer errors.

1.4 Objectives and limitations

The activities and objectives of the thesis form part of a project for development of a Proof of Concept Prototype managed by Tructric AB. The objective of this thesis is to develop the subsystems required for a reverse driver assist function. As illustrated in the concept system flowchart in Figure 1.3, the system consists of four main subsystems:

1. Vehicle localization using external sensors.
2. Path planner to generate a route that can be followed to reach the desired end conditions.
3. Path following controller to corrects driver inputs and ensure the vehicle tracks the planned path.
4. User interface for showing steering instructions to the driver.

Additionally, the overall design must use computationally simple methods to ensure real-time performance.

The limitations identified for the thesis are:

1. Implementation and testing to be done on one specific test vehicle (Volvo FHE).
2. Given the time constraints, the scope of the work was limited to the application of established methods.

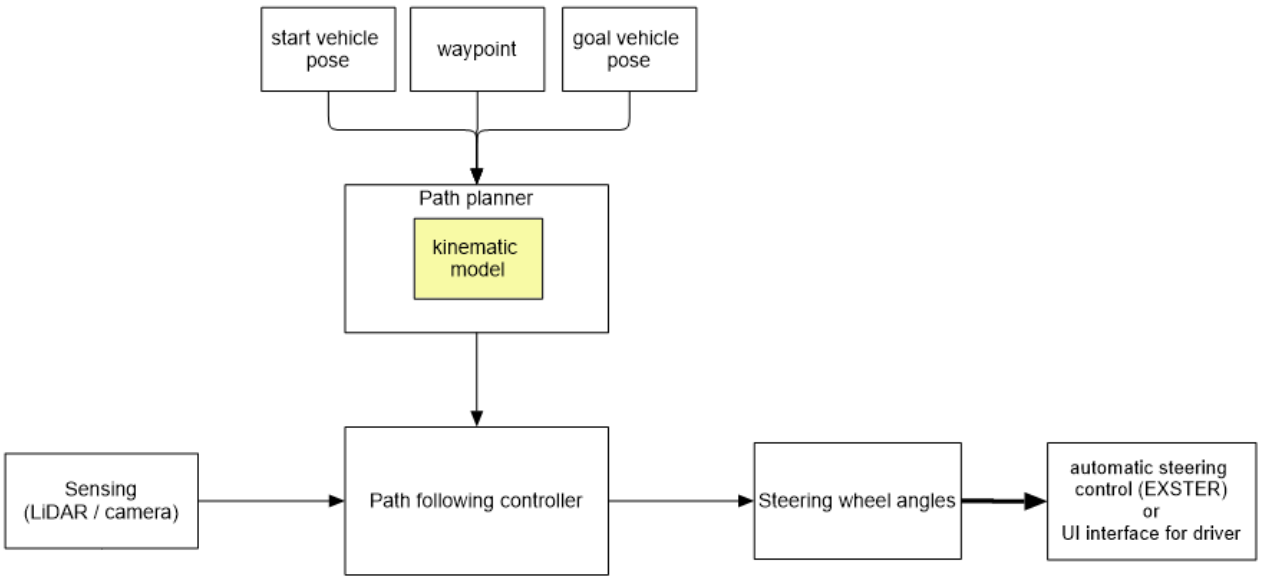


Figure 1.3: Concept flowchart

2
Sensing

To locate the truck and semi-trailer and to measure changes in their position and orientation, this thesis adopts the use of external sensors. This choice is made from the perspective of developing a solution that does not depend on proprietary or vehicle-specific onboard technology. Using external sensing, the approach remains applicable to most vehicles on the road today, not only to specially equipped test platforms.

For the system to plan or control the motion of the truck–trailer combination, it must know the vehicle's current position and orientation in the environment. This requires measuring or estimating geometric states that fully describe the motion of both units. The parameters of interest to be measured or estimated using sensors are:

1. Lateral position, longitudinal position and heading angle of truck.
2. Lateral position, longitudinal position and heading angle of semi-trailer.
3. Articulation angle of the combination.

This work considers three sensing technologies with distinct characteristics—LiDAR, radar, and camera-based vision—to evaluate which modalities best suit the requirements of the truck–trailer configuration. A comparison of these technologies is provided in Table. 2.1 including data that can be found in manuals and empirical observations:

Table 2.1: Sensing methods explored

Type	Equipment	Advantages	Challenges
LiDAR	Velodyne VLP-16 [9], VLP32C [10]	• Fine angular resolution (horizontal and vertical). • Structured position data. • Data size of each frame is small (75 to 120 KB).	• Partial occlusion, loss of sight of one unit. • Sparse datapoints at distance. • Material reflectivity issues. • Degraded performance in rain or fog.

Type	Equipment	Advantages	Challenges
RADAR	SmartMicro DRIVEGRD [11] or TRUGRD [12]	• Longer detection range. • Doppler velocity measurement. • Robust all weather performance.	• Lower angular resolution than LiDAR. • Multipath reflection from metallic objects.
Camera	AXIS P1375 IP camera [13]	• Lower equipment cost. • Large field of view.	• Performance degradation in extreme lighting conditions (glare, low light, etc.). • Calibration for position or angle detection requires large datasets. • Reliable algorithms often require neural network or ML. • Data size of each frame is comparatively large (200 to 900 KB for 720p).

For this thesis, Velodyne VLP-16 LiDAR was selected as it provides substantially higher spatial resolution than the available SmartMicro radar and delivers geometric measurements independent of illumination conditions, unlike a camera which is sensitive to lighting variability. Additionally, LiDAR recordings generate significantly smaller and more manageable datasets than camera video recordings. This enables efficient real-time processing, allowing the system to react quickly to changes in the vehicle pose.

2.1 Setup

Velodyne VLP-16 mounted on a tripod that can be set at vertical positions ranging from 0.5 m up to 1.8 m as shown in Figure 2.1. The LiDAR was powered by a portable 12V DC battery. The VLP-16 model specifications are listed in the Table 2.2.

Table 2.2: VLP-16 Specification

Device specification	Values [14]
channels	16
vertical FOV	$-15°$ to $+15°$
vertical resolution	$2°$
horizontal FOV	$360°$
horizontal resolution	$0.1°$ to $0.4°$

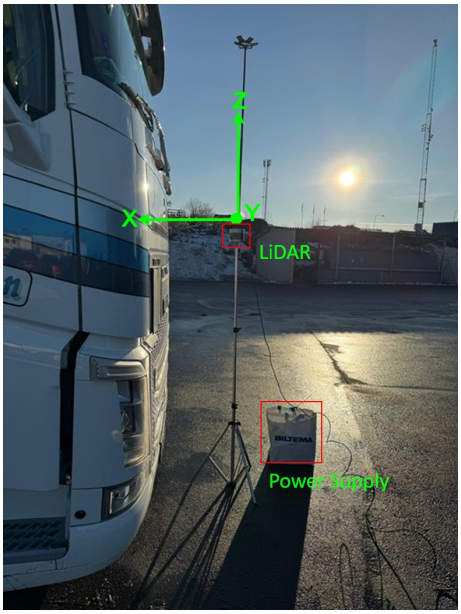
2.2 Field data gathering

To be able to build an algorithm to identify truck and trailer edges and estimate position, these factors were considered while picking locations to record passing trucks:

1. Slow speed driving (< 3 m/s)
2. Places where the road has curvature or areas where a truck and trailer move with non-zero articulation (cargo loading areas or ports) to capture trailer behavior.
3. Trucks moving within a 20 m radius of LiDAR.

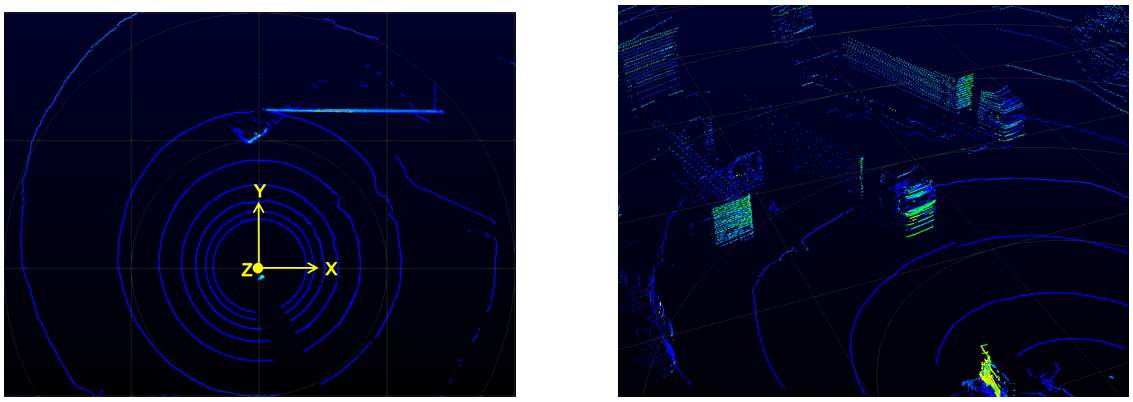


(a) Tripod mounted low



(b) Tripod maximum extension

Figure 2.1: LiDAR used to collect data



(a) Sample frame - top view **(b)** Sample frame - perspective view

Figure 2.2: Truck and trailer view from LiDAR recordings [15]

2.3 Methods and algorithms for point cloud processing

Widely used methods for identifying features or objects in images and LiDAR point clouds often include a combination of:

1. RANSAC (Random sample consensus) [16]
2. PCA (Principal component analysis) [17]
3. K-means clustering [18]
4. DBSCAN (Density-Based Spatial Clustering of Applications with Noise) [19]

However, when these methods were applied directly to the dataset, they did not produce reliable trailer detections.With K-means or DBSCAN clustering, the results were inconsistent. The LiDAR point cloud contained a high amount of noise, and using tight clustering parameters often caused parts of the object of interest to be excluded or fragmented into multiple clusters. This made the vehicle shape unstable and difficult to interpret.

Applying PCA or RANSAC after clustering to detect trailer edges also generated inconsistent output. Any line-like structure in the scene—such as road kerbs, fences, or other elongated objects were frequently interpreted as a trailer edge, leading to false detections.

The trailer detection logic proposed (Figure 2.3), tries to reliably track the trailer in an inherently noisy dataset (environment, people, other vehicles) and avoids the limitations of the above mentioned methods -in context of our motion scenario.

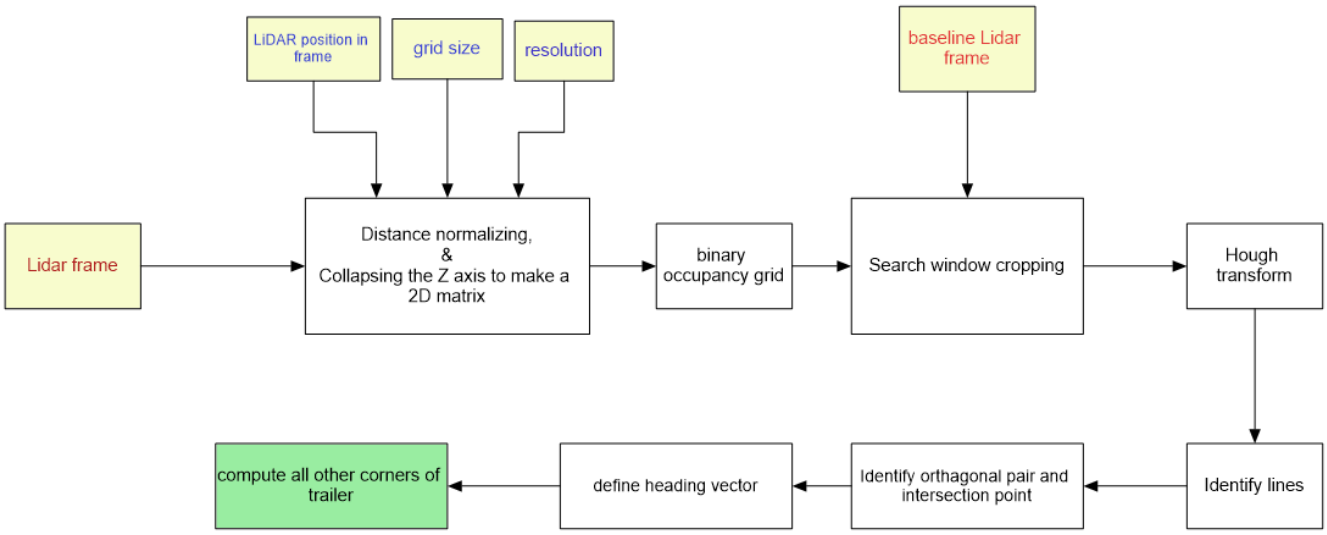
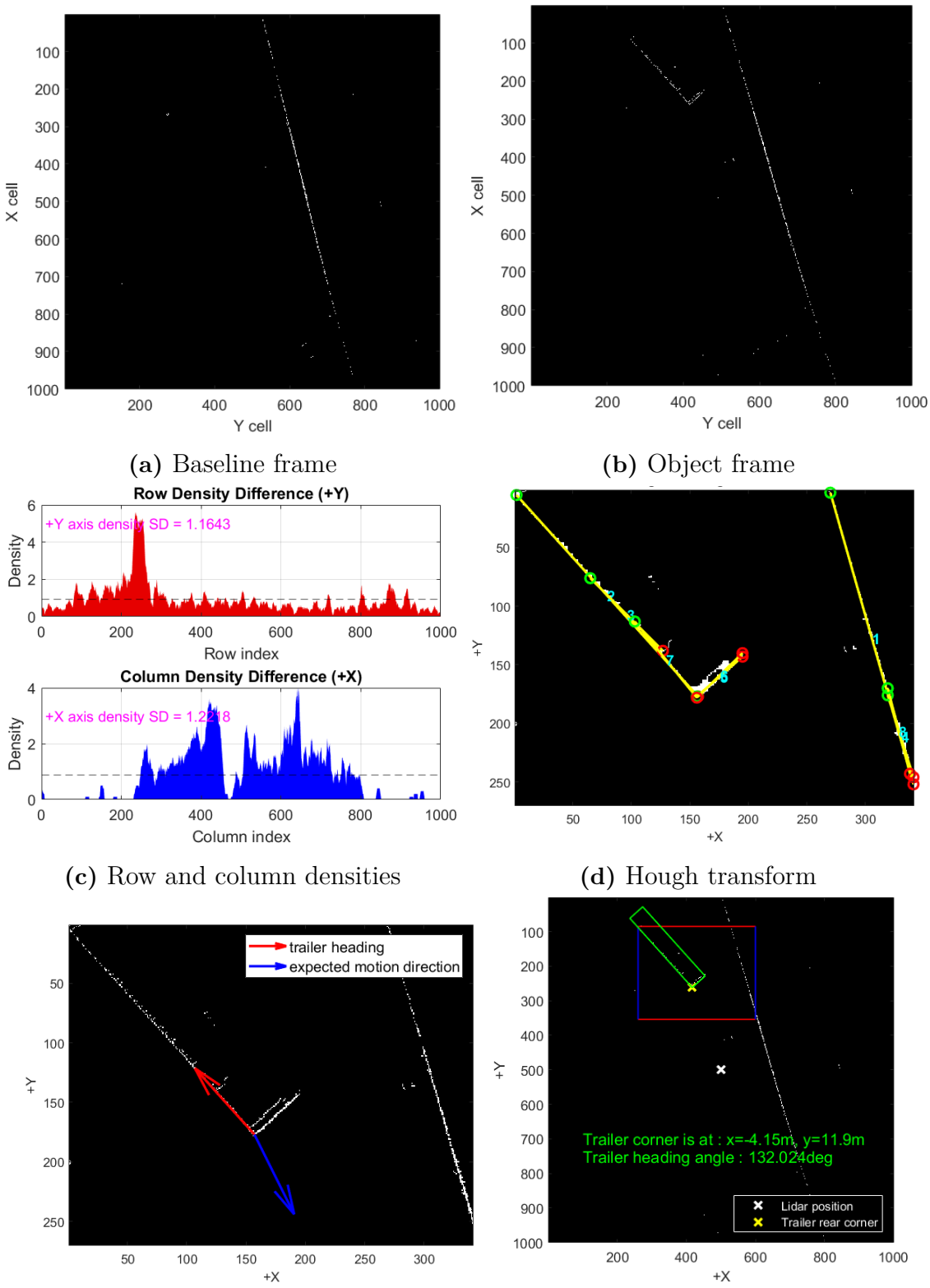


Figure 2.3: High-level overview of LiDAR sensing logic

The overview of the process, shown with an example frame in Figure 2.4:

1. Normalize LiDAR measurements such that sensor is always at the center of each frame.
2. Convert the point cloud into an occupancy grid to obtain a binary spatial representation (Figure 2.4a,2.4b).
3. Identify a search region by comparing row and column density changes against a baseline frame that contains only background structures (Figure 2.4c).
4. Apply a Hough transform within the search region to extract dominant line segments (Figure 2.4d).
5. Select orthogonal line pairs whose intersection forms a candidate trailer corner.
6. Assign a heading vector originating from the detected corner and oriented opposite to the direction of motion, representing the trailer's pose (Figure 2.4e).



(a) Baseline frame

(b) Object frame

(c) Row and column densities

(d) Hough transform

(e) Heading vector

(f) Search zone & bounding box

Figure 2.4: Localization using LiDAR point cloud

3

Modeling and Path planning

At low speeds (v < 2 m/s), slip angles and tire lateral forces can be assumed to be negligible. Under these conditions, a single track kinematic model with zero-sideslip assumption is known to provide sufficient accuracy for path planning and control applications[20][21].

The kinematic model when linearized about a straight-pose operating point, gives a linear time-invariant state-space representation. Within a limited operating domain, the kinematic model a provides a valid basis for LQR controller design. The primary trade-off of using a linearized kinematic model is that its validity deteriorates at large steering and articulation angles.

3.1 Kinematic Model

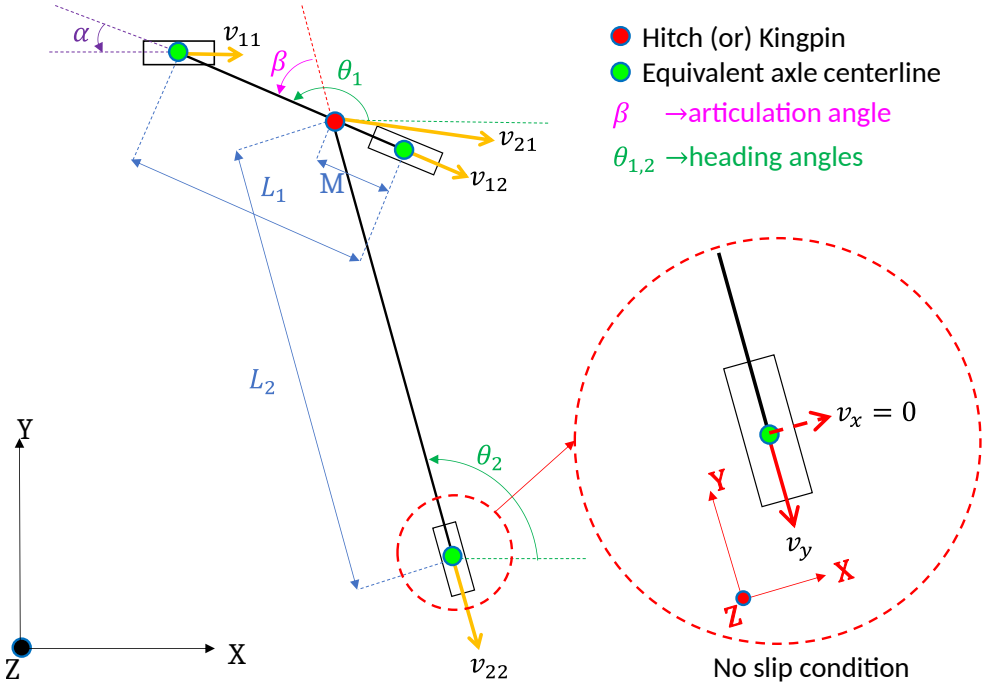


Figure 3.1: Kinematic model schematic (drawn for M<0)

The coordinate system for the planar motion of the model is the X-Y plane with the origin chosen in a way that all the motion is limited to the first quadrant only.

Angles are measured relative to the X axis (positive counterclockwise), as seen in Figure 3.1

The non-linear equations that describe the motion of the tractor and trailer in a single truck and semi-trailer with off axle hitch are:

$$\dot{X}_{12} = v_{12}\cos(\theta_1) \tag{3.1}$$

$$\dot{Y}_{12} = v_{12}\sin(\theta_1) \tag{3.2}$$

$$\dot{\theta}_1 = \frac{v_{12}}{L_1}\tan(\alpha) \tag{3.3}$$

$$\dot{\theta}_2 = \frac{v_{12}}{L_2}\left(\sin(\beta) - \frac{M\cos(\beta)\tan(\alpha)}{L_1}\right) \tag{3.4}$$

$$\beta = \theta_1 - \theta_2 \tag{3.5}$$

$$\dot{\beta} = \frac{v_{12}}{L_1 L_2}\left(L_2\tan(\alpha) - L_1\sin(\beta) + M\cos(\beta)\tan(\alpha)\right) \tag{3.6}$$

$$v_{22} = v_{12}\cos(\beta) + \frac{v_{12}M\sin(\beta)\tan(\alpha)}{L_1} \tag{3.7}$$

$$\dot{X}_{22} = v_{22}\cos(\theta_2) \tag{3.8}$$

$$\dot{Y}_{22} = v_{22}\sin(\theta_2) \tag{3.9}$$

The variables and conventions used are presented in Table 3.1.

Table 3.1: Variables and parameters of the kinematic single track model

Symbol	Description	Unit
X_{11}, Y_{11}	Position of the tractor front axle center	m
X_{12}, Y_{12}	Position of the tractor rear axle center	m
X_{21}, Y_{21}	Position of the hitch point or 'kingpin'	m
X_{22}, Y_{22}	Position of the trailer effective rear axle center	m
θ_1	Heading angle of the tractor relative to the X axis	rad
θ_2	Heading angle of the trailer relative to the X axis	rad
β	Articulation angle, $\beta = \theta_1 - \theta_2$	rad
α	Tractor front road wheel angle (input - positive for left steering,counterclockwise)	rad
v_{12}	Longitudinal velocity of the tractor rear axle center (input)	m/s
v_{22}	Longitudinal velocity of the trailer axle center	m/s
L_1	Tractor wheelbase (front axle to effective rear axle)	m
L_2	Trailer wheelbase (kingpin to effective rear axle centerline)	m
M	Hitch offset, longitudinal distance from tractor effective rear axle to kingpin (negative when the kingpin is ahead of the rear axle)	m

To minimize numerical error accumulation resulting from the integration of multiple state derivatives, the plant model is formulated using a reduced state vector comprising four states: $[X_{22}, Y_{22}, \theta_2, \beta]$. Kingpin, tractor rear axle, and front axle positions are then reconstructed algebraically, eliminating drift in those quantities.

$$\begin{bmatrix} \dot{X}_{22} \\ \dot{Y}_{22} \\ \dot{\theta}_2 \\ \dot{\beta} \end{bmatrix} = \begin{bmatrix} \left(v_{12}\cos(\beta) + \frac{v_{12} M \sin(\beta)\tan(\alpha)}{L_1}\right)\cos(\theta_2) \\ \left(v_{12}\cos(\beta) + \frac{v_{12} M \sin(\beta)\tan(\alpha)}{L_1}\right)\sin(\theta_2) \\ \frac{v_{12}}{L_2}\left(\sin(\beta) - \frac{M\cos(\beta)\tan(\alpha)}{L_1}\right) \\ \frac{v_{12}}{L_1 L_2}\left(L_2\tan(\alpha) - L_1\sin(\beta) + M\cos(\beta)\tan(\alpha)\right) \end{bmatrix} \tag{3.10}$$

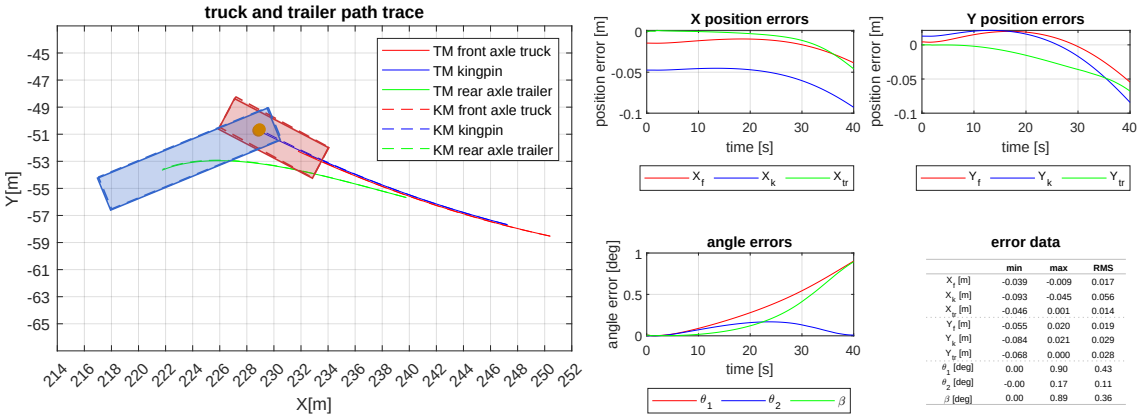
$$\begin{aligned} \text{Hitch (kingpin) position:} \quad & X_{21} = X_{22} + L_2\cos\theta_2 \\ & Y_{21} = Y_{22} + L_2\sin\theta_2 \\ \text{Tractor rear axle position:} \quad & X_{12} = X_{21} + M\cos\theta_1 \\ & Y_{12} = Y_{21} + M\sin\theta_1 \\ \text{Tractor front axle position:} \quad & X_{11} = X_{12} + L_1\cos\theta_1 \\ & Y_{11} = Y_{12} + L_1\sin\theta_1 \end{aligned}$$

3.1.1 Model validation using TruckMaker™ simulations

IPG TruckMaker [22] has a wide range of high fidelity vehicle models and the deviations from the dynamic simulations can help identify regions of validity of the kinematic model.

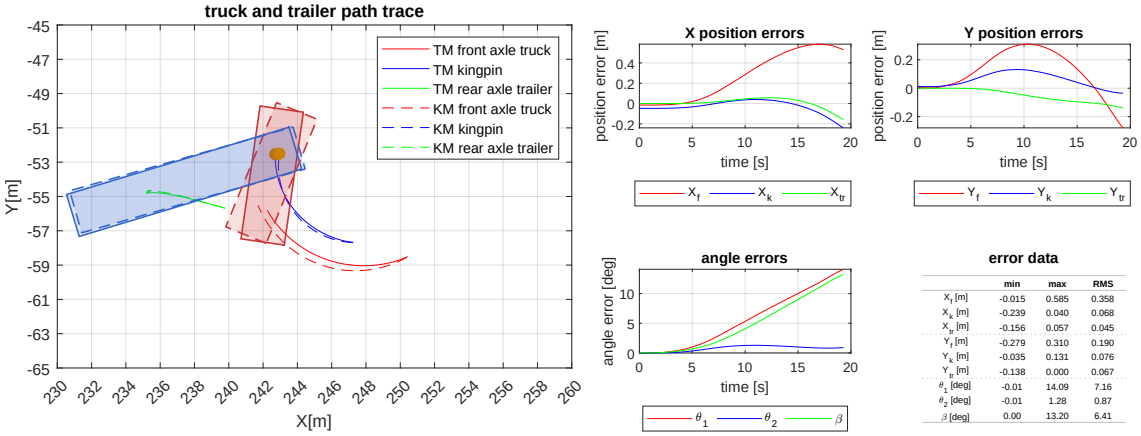
To validate the kinematic model TruckMaker was used to run constant velocity and constant steering maneuvers. The differences in trajectory are shown in Figure 3.2 which is a constant 1 rad handwheel angle and constant truck speed of 1 m/s in reverse. Figure 3.3 shows the behaviour of the single track model against TruckMaker model at a large handwheel angle of 12.5 rad, where solid lines indicate the output from TruckMaker simulation and dashed lines indicate kinematic model open loop simulation.

TruckMaker simulates a full multi body dynamic model, therefore mismatches and divergence between the paths are expected.



(a) Kinematic model vs. TruckMaker **(b)** Position and angle errors

Figure 3.2: Model validation with handwheel angle of 1 rad



(a) Kinematic model vs. TruckMaker **(b)** Position and angle errors

Figure 3.3: Model validation with handwheel angle of 12.5 rad

3.2 Computational methods for path planning

In this work, the reverse path planning task for the articulated vehicle is formulated under the following simplified conditions:

- Maneuver distance range upto a maximum of $40m$. - Focusing on the area close to the 'rail wagon' or target position in space.
- No obstacles considered in the movement path.
- Driving surface is perfectly flat.

3.2.1 Commonly used methods

Some of the relevant, commonly used methods for motion planning are briefly discussed in this subsection:

a) bvp4c solver

MATLAB's bvp4c function solves [23] two-point boundary value problem by enforcing the system's differential equations and boundary conditions simultaneously.While it works well for stable systems, it is not suitable for articulated vehicle path planning because:

- It is highly sensitive to the initial guess of the trajectory
- It struggles with non-holonomic constraints, which impose differential relations that cannot be freely integrated.
- The method frequently fails to converge to the required final pose.

Due to these limitations, bvp4c was not pursued further.

b) RRT

Rapidly-Exploring Random Trees (RRT) are widely used for navigation in cluttered environments because they efficiently explore the motion domain.However, for the present scenario RRT would produce non-smooth, jagged paths that require post-processing.

Without obstacles, the method provides no advantage over optimization-based planners. Thus, RRT was not selected as the primary method.

c) Hybrid A^*

Hybrid A^* combines grid-based search with continuous-state vehicle motion primitives.Some of the advantages of this method are:

- Ability to handle non-holonomic constraints
- Resolution-completeness i.e provided that a feasible trajectory exists within the chosen grid, the algorithm will eventually discover it.

However, for short, obstacle-free reverse maneuvers:

- The grid resolution must be very fine to achieve high accuracy and path smoothness.
- Post-smoothing is still required.

Hybrid A^* remains a strong candidate but was not necessary for the simplified scenario.

d) Direct collocation

Direct collocation solves an optimal control problem by discretizing both the state and control trajectories. System dynamics are then imposed as algebraic constraints at each discretization point, converting the differential equations into a finite-dimensional problem that can be handled by standard numerical optimization solvers.

The path planning problem for an articulated vehicle fits into this framework: given a start and goal pose, the task is to find a steering profile that drives the system between them while minimizing path length and respecting constraints. Discretizing over arc length rather than time decouples path geometry from vehicle speed, which is convenient for a system where speed is not planned but held approximately constant by the driver.

This method provides a good balance of accuracy, path smoothness, and computational efficiency for this particular scenario.

3.2.2 Direct collocation algorithm

The implementation of direct collocation for solving path planning in this case is done by defining a start pose X_s and goal pose X_g, where 'pose' is defined as a vector $[x, y, \theta_2, \beta]$.

The physical limits are defined by α_{max} for maximum road wheel steering angle and β_{max} for maximum allowed articulation angle. Weight terms W_{smooth} for steering rate and W_β for articulation angle are introduced, which are used in the cost function.
The geometric parameters L_1, L_2, M of the truck and semi-trailer are also defined (see Figure 3.1). An example of parameters and limits used as inputs for the solver are shown in Table 3.2. Note that these values are for the Ro-Ro maneuver with values chosen to suit the test vehicle.

Table 3.2: Selected parameter values used in the path planner

Parameter	Description	Selected value
N	Discretization points	60
X_s	Start pose	[115 m, 115 m, 67.5°, 0°]
X_g	Goal pose	[100 m, 92.3 m, 90°, −90°]
$\alpha_{\max}$	Maximum allowed road wheel angle	35°
$\beta_{\max}$	Maximum allowed articulation angle	90°
W_{smooth}	Penalty on steering rate	0.2
W_β	Penalty on articulation angle	0.1
L_1	Wheelbase of tractor	4.585 m
L_2	Distance from kingpin (hitch) to trailer lumped axle	7.700 m
M	Hitch point offset from tractor rear axle	−0.480 m

The method is presented in the form of a pseudo-code below where the cost function to be minimized is shown in equation 3.14.

Algorithm: Direct Collocation Solver for Tractor-Semi-trailer Path Planning

Input: Start pose X_s=$[x_s, y_s, \theta_{2s}, \beta_s]$, goal pose X_g=$[x_g, y_g, \theta_{2g}, \beta_g]$, model parameters (L_1, L_2, M), limits $(\alpha_{\max}, \beta_{\max})$, number of nodes N.
Here x and y denote the global position (X_{22}, Y_{22}) of the trailer effective axle center (Table 3.1).
Output: Optimized trajectory $(x, y, \theta_2, \beta, \alpha, S)$.

1. Construct decision vector z:

$$z = [x_1, \ldots, x_N,\ y_1, \ldots, y_N,\ \theta_{2,1}, \ldots, \theta_{2,N},\ \beta_1, \ldots, \beta_N,\ \alpha_1, \ldots, \alpha_N,\ S]. \tag{3.11}$$

2. Build initial guess z_0:

- Linear interpolation for x_i, y_i
- Wrapped interpolation for $\theta_{2,i}, \beta_i$
- $\alpha_i = 0$ for all i
- $S = S_{\text{init}}$

3. Define cost function $J(z)$:

$$ds = \frac{S}{N-1}, \tag{3.12}$$

$$\alpha'_i = \frac{\alpha_{i+1} - \alpha_i}{ds}, \tag{3.13}$$

$$J(z) = S + W_{\text{smooth}}\, ds \sum_{i=1}^{N-1} (\alpha'_i)^2 + W_\beta\, ds \sum_{i=1}^{N} \beta_i^2. \tag{3.14}$$

4. Define collocation constraints $ceq(z)$:
For each node $i = 1, \ldots, N$ (derivatives with respect to the tractor rear-axle arc length s, with $\sigma = \text{sign}(v_{12})$, i.e. $+1$ forward and -1 reverse):

$$\kappa_i = \frac{\tan(\alpha_i)}{L_1}, \tag{3.15}$$

$$\theta'_{1,i} = \sigma\, \kappa_i, \tag{3.16}$$

$$\theta'_{2,i} = \frac{\sigma \sin\beta_i - M \cos\beta_i\, \theta'_{1,i}}{L_2}, \tag{3.17}$$

$$v'_{2,i} = \sigma \cos\beta_i + M \sin\beta_i\, \theta'_{1,i}. \tag{3.18}$$

State derivatives:

$$f_i^x = v'_{2,i} \cos\theta_{2,i}, \tag{3.19}$$

$$f_i^y = v'_{2,i} \sin\theta_{2,i}, \tag{3.20}$$

$$f_i^{\theta_2} = \theta'_{2,i}, \tag{3.21}$$

$$f_i^\beta = \theta'_{1,i} - \theta'_{2,i}. \tag{3.22}$$

Trapezoidal collocation for each interval $i = 1, \ldots, N-1$**:**

$$x_{i+1} - x_i = \frac{ds}{2}(f_i^x + f_{i+1}^x), \tag{3.23}$$

$$y_{i+1} - y_i = \frac{ds}{2}(f_i^y + f_{i+1}^y), \tag{3.24}$$

$$\theta_{2,i+1} - \theta_{2,i} = \frac{ds}{2}(f_i^{\theta_2} + f_{i+1}^{\theta_2}), \tag{3.25}$$

$$\beta_{i+1} - \beta_i = \frac{ds}{2}(f_i^{\beta} + f_{i+1}^{\beta}). \tag{3.26}$$

Boundary constraints:

$$(x_1, y_1, \theta_{2,1}, \beta_1) = X_s, \tag{3.27}$$

$$(x_N, y_N, \theta_{2,N}, \beta_N) = X_g. \tag{3.28}$$

5. Solve nonlinear program:

$$\min_z \quad J(z) \tag{3.29}$$

$$\text{s.t.} \quad ceq(z) = 0, \tag{3.30}$$

$$\alpha_i \in [-\alpha_{\max}, \alpha_{\max}], \tag{3.31}$$

$$\beta_i \in [-\beta_{\max}, \beta_{\max}], \tag{3.32}$$

$$S > 0. \tag{3.33}$$

Use `fmincon` (interior-point) and adjust `MaxIterations`, `MaxFunctionEvaluations`, `ConstraintTolerance`, `OptimalityTolerance`, `StepTolerance` if needed.

6. Extract solution:

- $x_i, y_i, \theta_{2,i}, \beta_i, \alpha_i, S$
- Reconstruct hitch and front axle geometry

3.3 Path following control

For single unit vehicles without articulation, geometry based pure pursuit controller, Stanley controller, state error feedback based PID (Proportional–Integral–Derivative) or LQR (Linear Quadratic Regulator) can be applied as a single stage control.

For articulated vehicles, the above mentioned methods can still be applied for forward driving case - but for a reverse path following application a single stage controller would involve Model Predictive Control in which all included control objectives are considered simultaneously (lateral position tracking, trailer heading control and articulation angle control).

3.3.1 Controller Architecture

The control architecture that was opted for in this work follows the two-stage strategy proposed by Zhaohui Ge [24]. The approach combines a feedback LQR controller, acting on the trailer heading angle, the lateral error of the look-ahead point, and the articulation angle, with a feedforward term derived from the curvature of the reference path. This formulation gives a path-tracking controller suitable for multi-unit vehicle configurations.

Ge's controller was originally developed and validated for long combination vehicles (LCVs), demonstrating stability and tracking performance. In the current thesis, the same control structure is adopted to the specific configuration of a tractor and semi-trailer system.

4

Vehicle testing

4.1 Test vehicle setup

The truck available at REVERE lab is a Volvo FHE 6x4, named 'Elephant', seen in Figure 4.1 .



Figure 4.1: REVERE 'Elephant' [25]

External sensors mounted onto the test vehicle:

1. OxTS RT3000 v4 (GNSS sensors, one on the tractor and one on the semi-trailer)
2. Curtiss-Wright NRH27C angle sensor (to measure articulation angle at the hitch point)

Signals are accessed via the CAN bus using a Kvaser CAN adapter, which interfaces a computer with the vehicle's CAN network. When provided with DBC files for the relevant devices on the network, raw CAN frames are decoded into signal values and logged for analysis, giving access to wheel speed, steering angle, pedal position and other relevant signals.

During the timeline there was one test opportunity where the goal was to log the following data while performing a set of maneuvers (Table 4.1):

Table 4.1: Logged data for each maneuver

Quantity measured	**Unit**	**Coordinate system / Convention**	**Sensor used**
GNSS latitude and longitude	deg	WGS84 geodetic	OxTS RT3000 v4
GNSS heading angle	deg	ISO 8855: yaw from East, positive counterclockwise	OxTS RT3000 v4
Yaw rate	deg/s	yaw rate in intermediate system (Z up), positive counterclockwise	OxTS RT3000 v4
Lateral and longitudinal acceleration	$\mathrm{m\,s^{-2}}$	ISO 8855 intermediate system: X forward, Y left, gravity removed	OxTS RT3000 v4
Accelerator pedal position	% (0–100)	–	Accelerator pedal position sensor (onboard vehicle)
Tractor speed	km/h	Scalar, unsigned magnitude	Wheel-speed sensor (onboard vehicle)
Steering wheel angle	deg	Positive counterclockwise (left turn), zero at straight ahead	Digital steering-angle encoder (onboard vehicle)
Steering wheel turning rate	deg/s	Same sign as steering wheel angle	Digital steering-angle encoder (onboard vehicle)
Articulation angle	deg	Counterclockwise positive $\beta = \beta_{\mathrm{Ch2}} - 182.357°$	Curtiss-Wright NRH27C

4.2 EXSTER Interface

For actuation, the EXSTER interface [26], available on Volvo FHE, FME, and other variants, is the only external actuation method supported by the test vehicle. It enables the following control requests on the BB-CAN (Body Builder Controller Area Network):

- Steering angle request
- Second accelerator
- Request of forward, neutral and reverse gears
- Proportional braking with the service brakes
- Remote control of the parking brake
- Brake and park feature.

This control setup is supported by a pre-configured Simulink environment to generate CAN instructions that can be sent via Kvaser CAN adapter.

4.3 Objectives and limitations

A test was conducted to prepare for future demonstration of a proof of concept prototype and to observe the challenges in maneuvering with a full scale vehicle on a test site. A specific objective was to gather maneuver data related to the specific vehicle combination.

A part of this test was also to validate the reverse maneuver path generated by the offline path planner, as the path following controller could not be implemented for the test. This was done by feeding the steering wheel angles open loop, through a precomputed distance-based lookup table, to retrace the ideal planned trajectory. The challenges in implementation were:

1. Variance in the GNSS position data occurred because RTK (Real-Time Kinematic) correction, was not available for the entire duration of the test.
2. The logic used to integrate successive position differences in order to estimate the traveled distance accumulated large errors. As shown in the code snippet below, this prevented the steering-input lookup from being performed correctly.

```
function distance = fcn(lat, lon)
    persistent d lat_prev lon_prev;
    if isempty(d)
        d = 0;
        lat_prev = lat;
        lon_prev = lon;
    end

    dlat = (lat - lat_prev) * 111412; %lattitude factor for
       the location
    dlon = (lon - lon_prev) * cosd(lat) * 111412;
    step = sqrt(dlat^2 + dlon^2);

    % only accumulate if position actually changed
    if step > 0.001  % 1mm threshold
        d = d + step;
    end

    lat_prev = lat;
    lon_prev = lon;
    distance = d;
end
```

Any metric obtained by integrating a signal over time accumulates error, so using it as the lookup variable will eventually fail. This is especially true for noisy signals such as GNSS position - summing the successive position differences adds the measurement noise at every sample, so the estimated distance grows even when the truck is stationary.

A distance estimate from integrating wheel speed sensor measurements avoids

this noise accumulation, but has error sources of its own - slip of the driven wheels, and uncertainty in the effective rolling radius. In addition, wheel speed sensors typically lose resolution at very low speeds.

In future work, further tests will be done to validate the path planner implemented as a part of path following control.

5
Results and discussion

5.1 LiDAR

5.1.1 Results

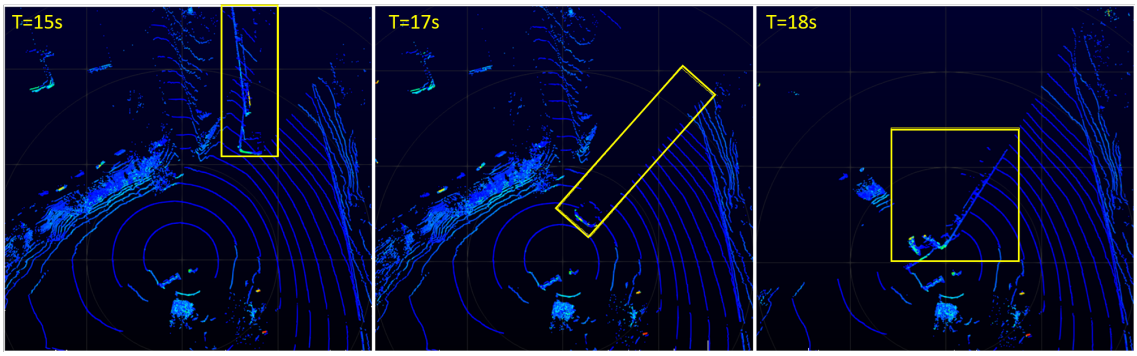
The proposed method achieved a trailer detection rate of approximately 70% when evaluated on recorded LiDAR recordings, outperforming the clustering-based approach. Although a 70% per-frame detection rate leaves room for missed detections, the high sampling rate of the VLP-16 LiDAR means that position and heading estimates are refreshed frequently, reducing the practical impact of individual missed frames on the overall pose estimate.

It is to be noted that with the LiDAR positioned near the test platform (to simulate mounting on a railway wagon), the LiDAR returns from the truck were sparse or non-existent. But when placed further away perpendicular to the parking area, it can be used to localize the tractor as well.

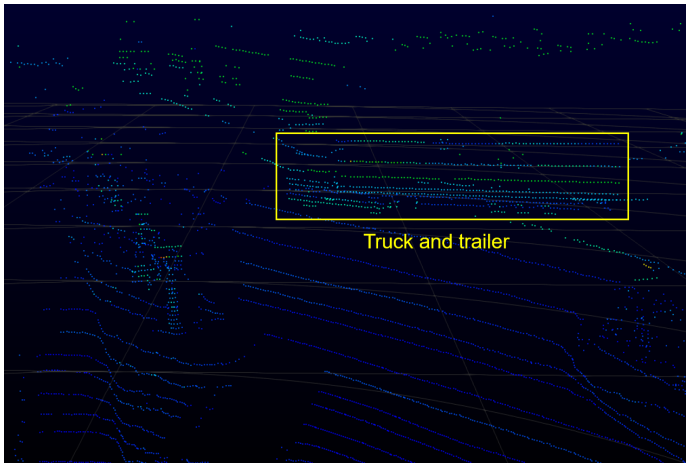
5.1.2 Challenges

With a statically mounted LiDAR the main challenges faced were:

1. Occlusion and shadows blocking parts of the truck and the trailer (Figure 5.1a).
2. At larger distances, the physical separation of reflection points creates a lower density of return points (Figure 5.1b).
3. Discontinuities and scattering depending on surface finish and material of target.



(a) Sample frame 1 - occlusion seen from top view



(b) Sample frame 2 - reduced return density at large distances

Figure 5.1: Annotated view of a truck and trailer, illustrating challenges in LiDAR-based perception

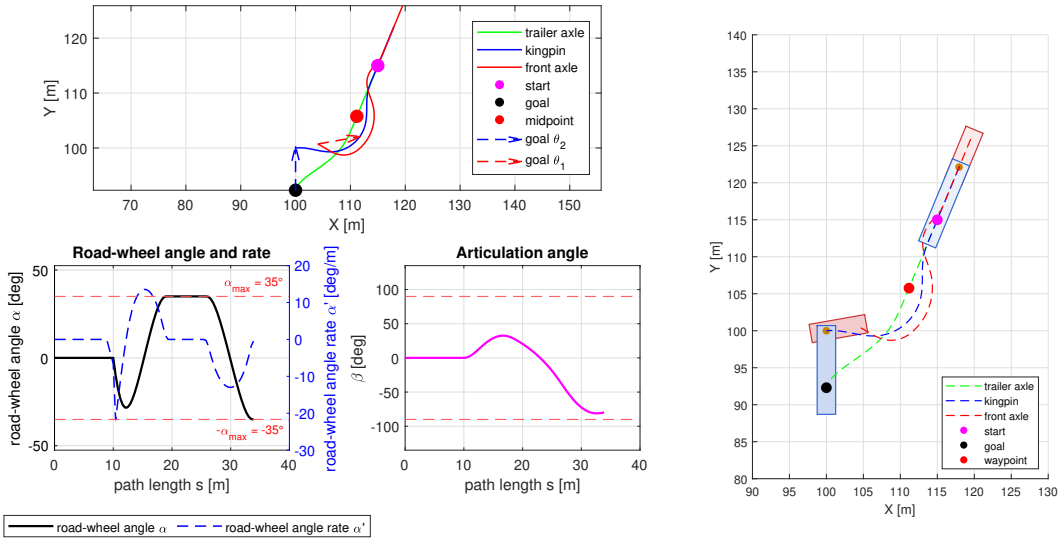
5.2 Path planner

5.2.1 Output

The spatial resolution of the planned path is determined by the number of discretized nodes N distributed over the total arc length S, giving a node spacing of

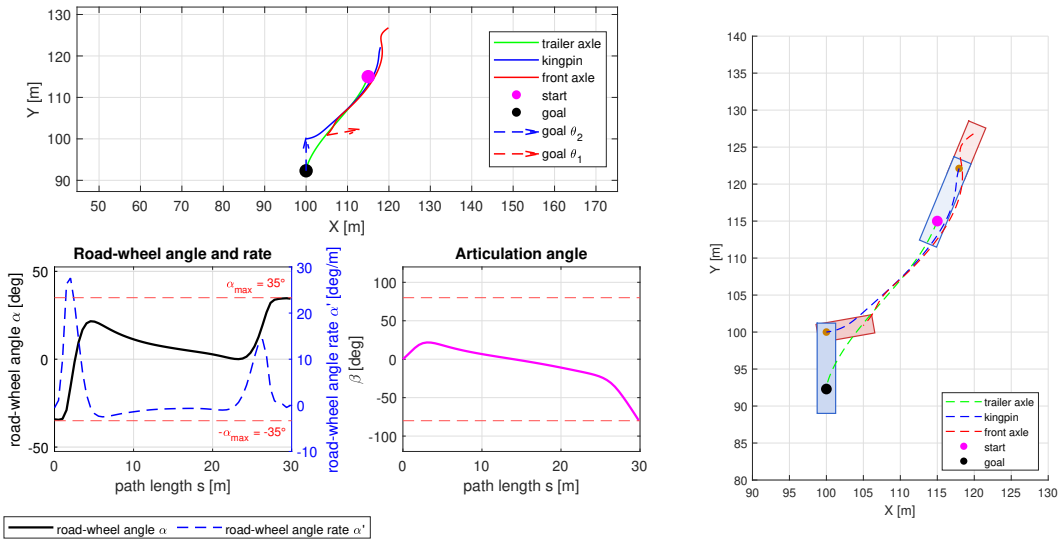
$$\Delta s = \frac{S}{N-1}$$

For maneuver distances up to 40 m, $60 \leq N \leq 80$ was found empirically to provide a node spacing of approximately 0.5–0.7 m, which is sufficient to produce continuous steering profiles without abrupt changes. The time complexity increases if a waypoint is introduced since it treats it as optimization problem for 2 path segments. The output is visually shown in Figure 5.2 and Figure 5.3 and further summarized in Table 5.1.



(a) Road-wheel angle,rate and articulation angle **(b)** Vehicle poses along path

Figure 5.2: Path planner output with way-point



(a) Road-wheel angle,rate and articulation angle **(b)** Vehicle poses along path

Figure 5.3: Path planner output without way-point

Table 5.1: Comparison of path planner performance with and without way-point

Parameter	**With way-point**	**Without way-point**
N	60	60
Max $\|\alpha\|$ [deg]	35.0	34.6
Max $\|\beta\|$ [deg]	81.1	80.0
Total S [m]	33.9	29.78
Computation time [s]	10.7	2.052

5.3 Path following controller

The controller's functioning was tested with a kinematic vehicle model in Simulink environment and not on the actual test vehicle yet, so some deviations in the path tracking performance are to be expected when implemented on a real vehicle.

5.3.1 Extending reference path

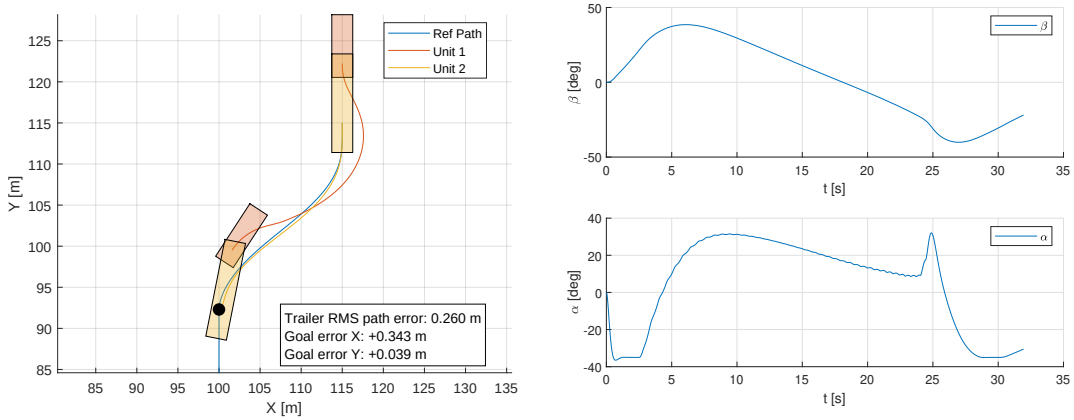
Since the vehicle stops when the look-ahead point has no further reference path, the output from the path planner has appended by adding a 'dummy' length that equals the look-ahead distance from the rear of the trailer as shown in an example in Figure 5.4.



Figure 5.4: Padding added to trailer reference path

5.3.2 Look-ahead distance and stability

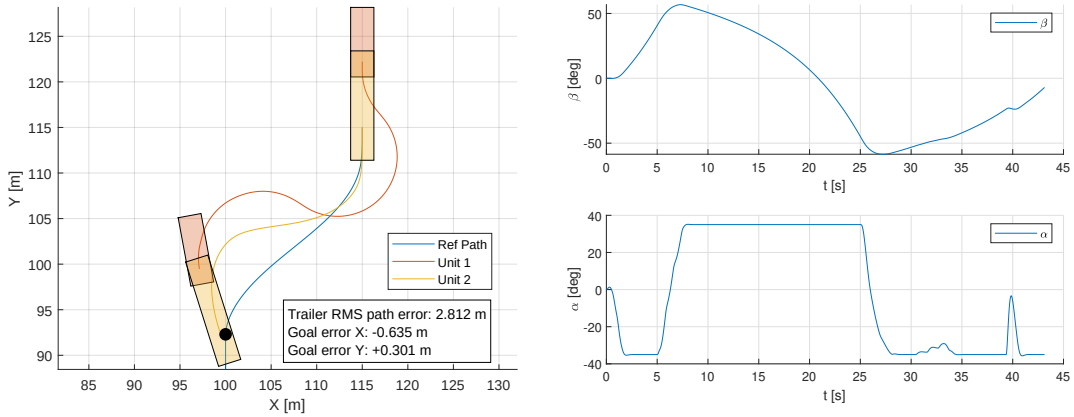
The look-ahead distance is a parameter that controls the trade-off between path tracking accuracy and control effort. Empirically, a look-ahead distance around 7.7m provides a balanced response (Figure 5.5), but reducing the value of this parameter (Figure 5.6) is shown to provide more aggressive steering inputs and potentially causing instability. Alternatively, increasing the look-ahead distance (Figure 5.7) is shown to reduce the path-tracking accuracy, resulting in non-convergence of trailer position to the goal.



(a) Tracking with look-ahead distance of 7.7m

(b) Articulation angle and steering input plot

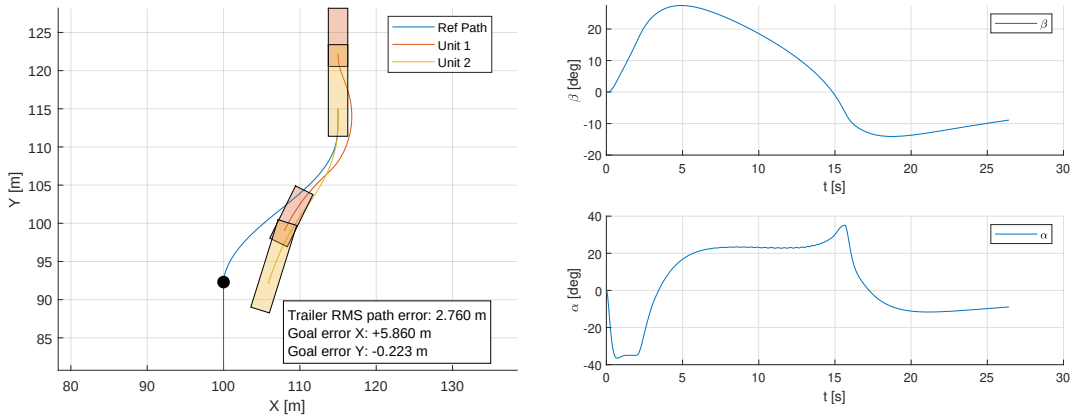
Figure 5.5: Example of path tracking performance with balanced look-ahead distance



(a) Tracking with look-ahead distance of 3.85m

(b) Articulation angle and steering input plot

Figure 5.6: Example of path tracking performance with shorter look-ahead distance



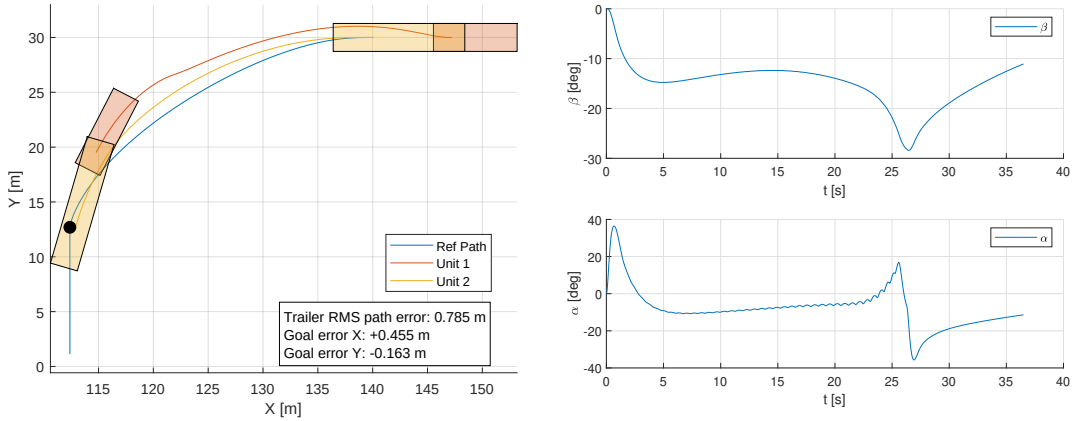
(a) Tracking with look-ahead distance of 11.5m

(b) Articulation angle and steering input plot

Figure 5.7: Example of path tracking performance with longer look-ahead distance

5.3.3 Articulation angle control

With the current setup the articulation angle requested at the end pose X_{goal} is not achieved, although the simulated vehicle model with the controller converges close to the target point. In the example shown in Figure 5.8 the start and goal conditions were: `X_start = [140, 30, 0°, 0°] and X_goal = [112.39, 12.69, 90°, -90°]`



(a) Tracking with look-ahead distance of 11.5m

(b) Articulation angle and steering input plot

Figure 5.8: Convergence of rear axle to target point

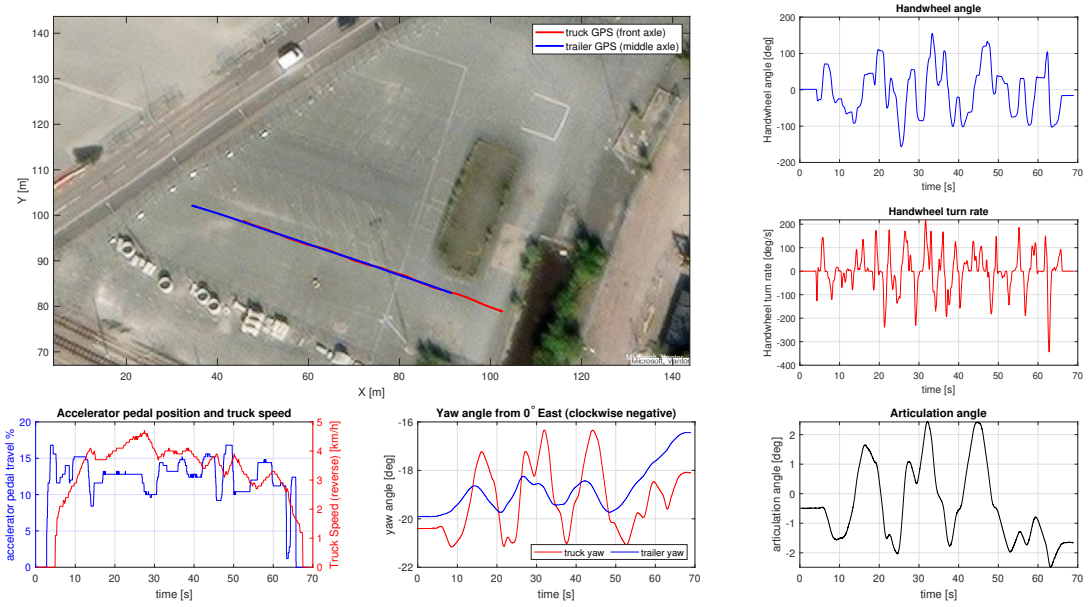
5.4 Outcomes of Testing

For the maneuvers performed during testing, the driver was required to operate the vehicle manually with the exception of the constant-steering-angle maneuvers, for which the steering actuation signals were successfully sent through Simulink interface to EXSTER. The driver was instructed to stop close to the jackknife point.

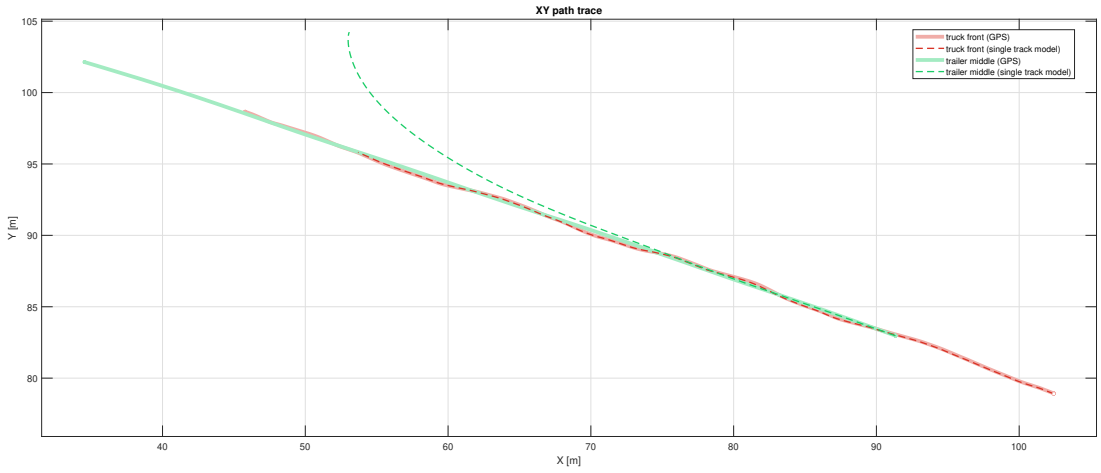
Regardless of not being able to automate the Ro-Ro parking maneuver during the test, the logged data is still useful for performing a black-box system identification based on input and output signals and to compare the real vehicle system with kinematic vehicle model.

The maneuvers performed included variations of:

1. Manual straight line reverse (Figure 5.9).
2. Constant steering angle reverse until close to jackknife (Figure 5.10).
3. Manual parking maneuver to position the trailer onto a platform to simulate the Ro-Ro maneuver on a rail wagon (Figure 5.11).



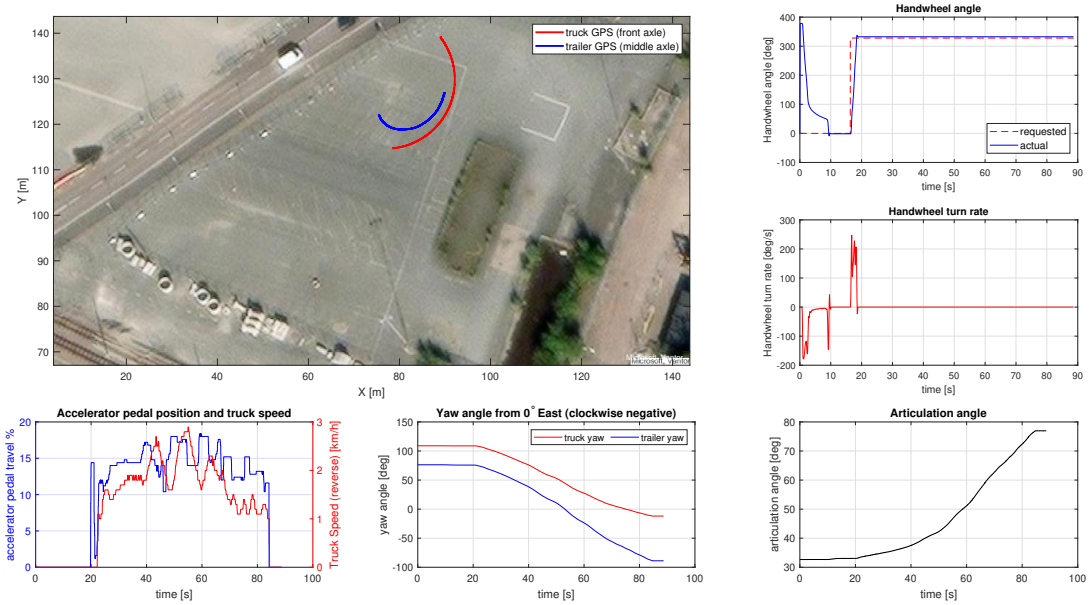
(a) Manual straight line reverse (logged data)



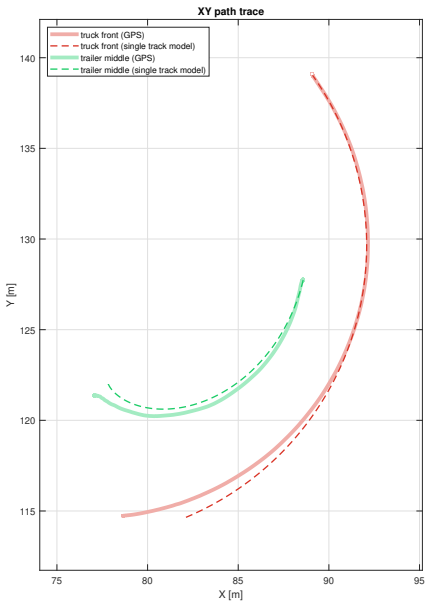
(b) Comparison of logged position data with kinematic model

Figure 5.9: Manual straight line reverse

The sensor data logged from straight line reversing maneuvers (Figure 5.9a) illustrate the steering action required to maintain the truck and trailer in a straight line. The kinematic single track model diverges eventually because it is an inherently unstable system in reverse, as seen in the truck and trailer path trace (Figure 5.9b).



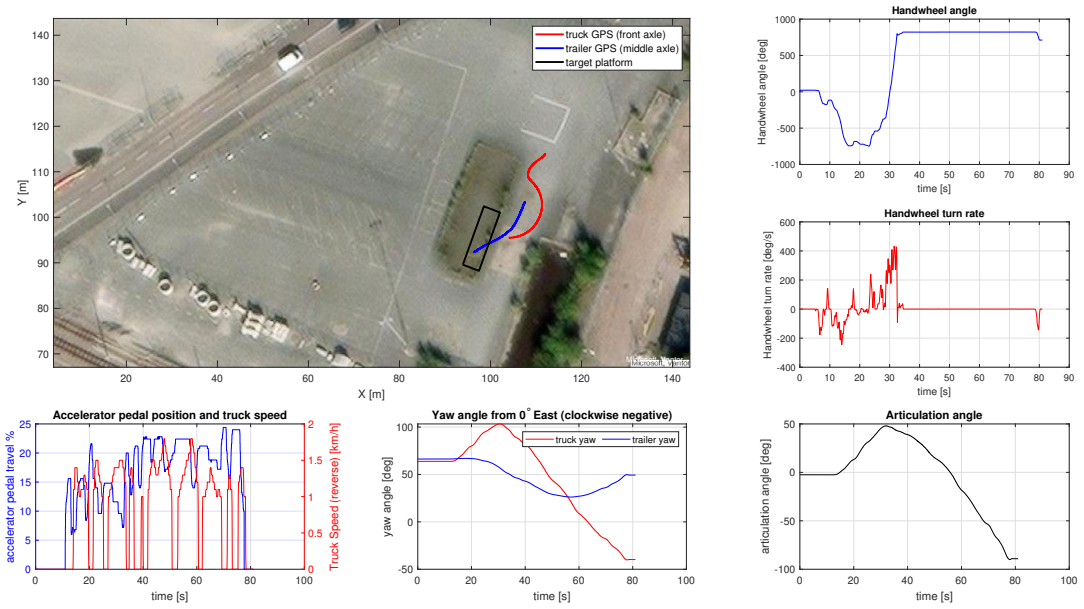
(a) Constant steering angle reverse (logged data)



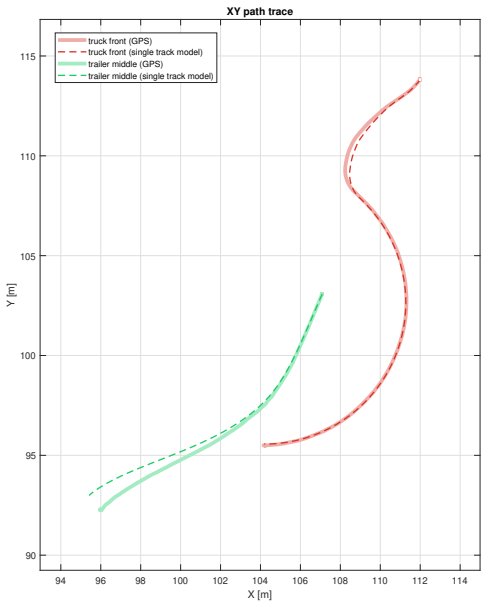
(b) Comparison of logged position data with kinematic model

Figure 5.10: Constant steering angle reverse close to jackknife

Constant steering angle maneuvers were performed over a range of values via a Simulink interface of EXSTER. The comparision of the single track kinematic model against the logged position data is shown in Figure 5.10b.



(a) Manual platform parking maneuver (logged data)



(b) Comparison of logged position data with kinematic model

Figure 5.11: Simulated Ro-Ro parking on test platform

The Ro-Ro parking maneuver was performed manually without external steering requests. Figure 5.11a shows the intended parking target area and the goal kingpin position. Figure 5.11b shows the tracking performance of open loop simulation of the kinematic single track model against the GPS position trace of the test truck and traile. Some deviations were observed even under the no slip assumption and low speed driving, presented in Table 5.2.

Table 5.2: RMS of position errors

Parameter	**Truck**	**Trailer**
X $\text{error}_{\text{rms}}$ (m)	0.089	0.257
Y $\text{error}_{\text{rms}}$ (m)	0.066	0.364
$\text{error}_{\text{X}_{\text{end position}}}$ (%)	0.4	5.1
$\text{error}_{\text{Y}_{\text{end position}}}$ (%)	−0.4	−6.8

This further emphasizes the importance of design and tuning of a path following controller instead of open loop, real-time vehicle model simulation, if the error at the endpoints have to be minimized further.

6
Conclusion and future work

6.1 Conclusion

This thesis proposes a framework demonstrating that a proof-of-concept driver assistance system for precision reverse manoeuvring of a truck–trailer combination can be built using established methods in sensing, path planning, and control.

A LiDAR-based perception pipeline was developed to estimate the pose of the trailer from a stationary external sensor, using geometric classification to identify the trailer's position and heading from sparse point cloud data.

A kinematic single-track model of the articulated vehicle was validated against TruckMaker simulations, forming the basis for a path planner implemented as a direct collocation nonlinear optimization problem. The planner reliably produces feasible, smooth paths from arbitrary start poses to a defined goal pose while respecting steering and jackknife constraints. A modified pure pursuit controller was implemented to follow the planned path in real time, taking the vehicle's estimated pose as input and outputting a road-wheel angle command, which can either be translated to the test truck's steering ratio and sent directly as control input or displayed as guidance to the driver.

The main limitations observed are the sensitivity of path tracking performance of the controller to look-ahead distance tuning and the inability of the current controller to reliably achieve the requested terminal articulation angle. Taken together, the work provides a technical foundation for a deployable reverse maneuvering aid, pending further tests to validate the real time functioning of the complete system.

6.2 Future Work

It is important that the complete process from vehicle pose identification, path planning and path following control are tested further to prove feasibility in real time operation. The other targeted works following this thesis are briefly discussed.

6.2.1 Terminal articulation angle control

In this implementation of the path following controller, the articulation angle is not weighted as a control objective. The articulation angle at the goal is therefore not controlled directly, but results from how the trailer follows the reference path. To keep the look-ahead point defined beyond the goal, the reference path is extended by a straight segment, and following a straight segment in reverse corresponds to zero articulation. As the look-ahead point reaches this extension, the controller begins to straighten the combination before the trailer reaches the goal, so the planned terminal articulation angle is not achieved.

Future work should revisit the extension of the planned reference path, for example by continuing the path along its final curvature instead of a straight line in the XY plane. The articulation angle could also be included as a weighted control objective. A further option is to gain-schedule the controller, using models linearized at different articulation angles up to those expected near the goal.

6.2.2 Improvements in LiDAR processing

The current trailer-detection pipeline operates on offline PCAP (Packet Capture) recordings, but future work should extend the system to real-time operation by decoding individual LiDAR packets or sampling complete frames as they are received.

6.2.3 Camera based identification and position estimation

Although the current system relies primarily on LiDAR for tractor and trailer pose estimation, future work should investigate a complementary machine-vision pipeline capable of detecting the tractor, trailer, and articulation geometry from camera data.

An image-processing module would provide an independent fallback sensing mode and enable sensor fusion with LiDAR, improving resilience in cases of occlusion, sparse point returns, or poor surface reflectivity. Ensuring the pose estimation is reliable under varying conditions represents an important step toward a more deployment-ready system.

6.2.4 User interface

A dedicated driver-guidance interface is required to convey steering instructions and real-time feedback on:

- Vehicle position relative to the planned path.
- Articulation angle.

- Steering sequence or recommended steering corrections.
- Deviation warnings when the driver drifts from the intended maneuver.

A mobile device (phone or tablet) connected via a local wireless network (Wi-Fi Direct or dedicated Hotspot) can serve as the baseline hardware platform. This avoids dependence on OEM displays and makes the system deployable across almost every tractor-trailer combination, independent on the model, or the production year.

Bibliography

[1] 'Transport emission data and projections' [Online].Available: https://panorama-sweden.com/?id=e69027c9-0390-487e-ad3f-c77b332837e5

[2] 'Fossilfritt Sverige'[Online]. Available: https://fossilfrittsverige.se/en/roadmap/the-automotive-industry-heavy-transport/

[3] 'Road transport data Sweden'[Online]. Available: https://www.trafa.se/en/road-traffic/swedish-road-goods-transport/

[4] RailFreight, 'Future loading units in European combined transport: What is the role of the semi-trailer?,' 2026. [Online]. Available: https://www.railfreight.com/intermodal/2026/02/09/future-loading-units-in-european-combined-transport-what-is-the-role-of-the-semi-trailer/.

[5] 'Reach Stacker | Wikimedia Commons.' [Online]. Available: https://commons.wikimedia.org/wiki/File:Kalmar_Peinemann_reachstacker_(1).jpg

[6] 'DCT Gdańsk – suwnica | Wikimedia Commons.' [Online]. Available: https://commons.wikimedia.org/wiki/File:DCT_Gda%C5%84sk_%E2%80%93_suwnica.JPG

[7] H. Hallesius, B. Kordnejad, and I. Nordmark, 'A pre-study for a new efficient transshipment technology for combined transports Public report' 2023. Available: https://www.vinnova.se/globalassets/mikrosajter/ffi/dokument/slutrapporter-ffi/cyklar-och-andra-fordon-rapporter/2023-00040engelska.pdf.

[8] Z. Ge, F. Bruzelius, and B. Jacobson, 'Challenges and opportunities of using rearview dynamic guidelines to assist articulated vehicles in reversing' Chalmers University of Technology, Gothenburg, Sweden.

[9] VLP16 datasheet. [Online].Available: https://docs.clearpathrobotics.com/assets/files/clearpath_robotics_029029-TDS2-00b7913d65b51a841cb5dc6c2b711487.pdf

[10] VLP32C datasheet. [Online].Available: https://www.mapix.com/wp-content/uploads/2018/07/63-9378_Rev-D_ULTRA-Puck_VLP-32C_Datasheet_Web.pdf

[11] DRVEGRD datasheet. [Online].Available: https://www.smartmicro.com/wp-content/uploads/2026/03/DRVEGRD_171_Automotive_Data_Sheet.pdf

[12] TRUGRD datasheet. [Online].Available: https://www.smartmicro.com/wp-content/uploads/2026/02/TRUGRD_UMRR-12-Type-48_Traffic-Management_Datasheet-1.pdf

[13] AXISP1375 datasheet. [Online].Available: https://www.axis.com/dam/public/4b/aa/7b/datasheet-axis-p1375-network-camera-en-US-336590.pdf
[14] Velodyne LiDAR, Inc., 'Puck: High-Definition 3D LiDAR Sensor', 63-9229 Rev-F, datasheet, 2015. [Online]. Available: https://www.hypertech.co.il/wp-content/uploads/2015/12/63-9229_Rev-F_Puck__Spec_Sheet_Web.pdf
[15] 'Veloview | Kitware ParaView.' [Online]. Available: https://www.paraview.org/veloview/
[16] MathWorks, 'RANSAC' [Online]. Available: https://se.mathworks.com/discovery/ransac.html
[17] MathWorks, 'PCA' [Online]. Available: https://se.mathworks.com/help/stats/principal-component-analysis-pca.html
[18] MathWorks, 'k-means clustering' [Online]. Available: https://se.mathworks.com/help/stats/k-means-clustering.html
[19] MathWorks, 'DBSCAN clustering' [Online]. Available: https://se.mathworks.com/help/stats/dbscan-clustering.html
[20] O. Ljungqvist, 'Motion Planning and Stabilization for a Reversing Truck and Trailer System', Dissertation, 2015.
[21] O. Ismail, 'Planning Method for a Reversing Single Joint Tractor-Trailer System', Dissertation, 2021.
[22] 'TruckMaker | IPG Automotive.' [Online]. Available: https://www.ipg-automotive.com/en/products-solutions/software/truckmaker/
[23] 'bvp4c function |Mathworks' [Online].Available: https://se.mathworks.com/help/matlab/ref/bvp4c.html?s_tid=srchtitle_support_results_1_bvp4c
[24] Z. Ge, 'On the challenges of reversing multi-articulated vehicles' Chalmers University of Technology, Gothenburg, Sweden, Mar. 2026 Available: https://research.chalmers.se/publication/550536/file/550536_Fulltext.pdf
[25] GU, 'Superspännande "Hack a truck" med hårfint avgörande '.[Online].Available: https://www.gu.se/nyheter/superspannande-hack-a-truck-med-harfint-avgorande.
[26] Volvo Trucks, 'Volvo Bodybuilder Instructions'. [Online].Available: https://vbi.truck.volvo.com/index.php.

DEPARTMENT OF MECHANICS AND MARITIME SCIENCES
CHALMERS UNIVERSITY OF TECHNOLOGY
Gothenburg, Sweden
www.chalmers.se



CHALMERS
UNIVERSITY OF TECHNOLOGY